Time resolved four- and six-wave mixing in liquids. II. Experiments

Steffen, T.; Duppen, K.

Published in:
Journal of Chemical Physics

DOI:
10.1063/1.473106

Time resolved four- and six-wave mixing in liquids. II. Experiments

Thomas Steffen, and Koos Duppen

Citation: The Journal of Chemical Physics **106**, 3854 (1997); doi: 10.1063/1.473106
View online: https://doi.org/10.1063/1.473106
View Table of Contents: http://aip.scitation.org/toc/jcp/106/10
Published by the American Institute of Physics

Time resolved four- and six-wave mixing in liquids. II. Experiments

Thomas Steffen and Koos Duppen
Ultrafast Laser and Spectroscopy Laboratory, Department of Chemical Physics, Materials Science Center, University of Groningen, 9747 AG, The Netherlands

(Received 16 September 1996; accepted 9 December 1996)

Femtosecond four- and six-wave mixing is employed to study intermolecular motion in liquids, using CS_2 as a working example. Nonresonant four-wave mixing yields the total spectral response associated with the low-frequency motions in the liquid. The results of optical Kerr effect and transient grating scattering experiments can be modeled equally well by homogeneously and inhomogeneously broadened intermolecular vibrations. Femtosecond nonresonant six-wave mixing, where two independent propagation times can be varied, contains a temporally two-dimensional contribution that provides information on the time scale(s) of these intermolecular dynamics. The six-wave mixing signal of CS_2 shows distinctly different behavior along the two time variables. When the first propagation time is varied, both librational motion at short times and a picosecond diffusive tail are observed. Along the second propagation time, there is no sign of diffusive response and the signal is solely determined by the librational motions. Its shape depends on the first propagation time, when it is varied between 0 and 500 fs, but it is unaffected by further increase of that delay. This is a strong indication for a finite correlation time of the fluctuations in the intermolecular potentials. The interplay between the initial coherent motions and the diffusive behavior on longer time scales is far from clear. A widely used model in which these are treated as independent harmonic processes fails to describe the results. © *1997 American Institute of Physics.* [S0021-9606(97)51610-2]

I. INTRODUCTION

Since the advent of femtosecond laser pulses[1–3] with durations much shorter than intra- or intermolecular vibrational periods, ultrafast nuclear motions in liquids have been probed by a number of time-domain spectroscopies. Impulsive nonresonant Raman scattering has been among the most powerful of these techniques, since it allows for the direct observation of vibrations in real time with a time resolution of 10 fs or less. In particular the (heterodyned) optical Kerr effect[4–6] (OKE) and transient grating scattering[7,8] (TGS) have been widely used to study inter- and intramolecular motions in a variety of neat liquids and binary mixtures.

Although these are third-order nonlinear experiments from the point of view of the optical interactions, the molecular dynamics that is probed is linear, in the sense that a single time variable suffices to describe the evolution of the system. This can be expressed in the form of a one-time correlation function, whose Fourier transform gives the spectrum of nuclear motion that is probed by the short laser pulses.[9] The information content is therefore in principle identical to that of spontaneous or stimulated frequency-domain Raman techniques.[10,11]

The spectrum of molecular motion cannot be directly interpreted in terms of a microscopic model for the dynamics, since there is no information on the time scale(s) of the various processes that give rise to the optical response. Part of the spectral width may be caused by *motion* of individual molecules or ensembles of molecules, but the spectrum may also reflect a distribution of local *environments* in the liquid. These processes are often modeled as homogeneous and inhomogeneous line broadening when the fast (homogeneous) and static (inhomogeneous) modulation limits hold for the coupling of the motional system with its surroundings. When the coupling occurs over a wide distribution of time scales, the dynamics has to be treated in the intermediate (non-Markovian) modulation limit.[12,13]

The time scale(s) of the molecular dynamics in liquids can only be characterized by methods in which multi-time correlation functions of the motion are probed.[9] This can, for instance, be accomplished by performing echo-type experiments that are capable of dissecting and identifying the various contributions to a line shape, caused by processes that occur on different time scales.[14,15] The Raman-version of the two-pulse photon echo, a seventh-order nonlinear effect, has recently been applied to study the dynamics of high-frequency intramolecular vibrations in liquids.[16–18]

A number of time-resolved fifth-order nonlinear experiments has also been reported. Examples are a Raman-grating experiment, designed to measure the life times of intramolecular vibrations,[19] a second-order CARS experiment, to study the dephasing of overtones of intramolecular vibrations,[20] and an IR pump incoherent anti-Stokes probe experiment, to explore intramolecular energy redistribution.[21] A few years ago, Tanimura and Mukamel predicted that a temporally two-dimensional fifth-order experiment could be used to obtain information on the time scales of intermolecular dynamics in liquids.[22] The principle of this experiment is shown in Fig. 1. Time T_1 after a first pulse pair excited all Raman-active molecular motions, accessible within the broad bandwidth of femtosecond laser pulses, a second pulse pair interacts with the propagating nuclear system, generating a complicated mixture of motional (quantum) states. After a second propagation time T_2 a probe pulse

 0021-9606/97/106(10)/3854/11/$10.00

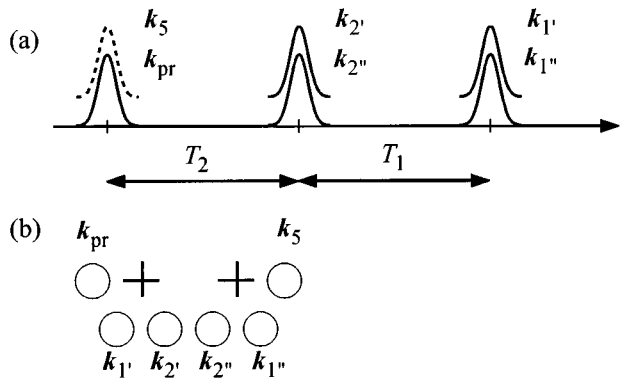

FIG. 1. (a) Principle of a two-dimensional nonresonant fifth-order experiment. Initially, two laser pulses with wave vectors $\mathbf{k}_{1'}$ and $\mathbf{k}_{1''}$ impulsively induce coherent nuclear motion. After a variable delay T_1 a second pulse pair with wave vectors $\mathbf{k}_{2'}$ and $\mathbf{k}_{2''}$ changes the nuclear state of the sample. Finally, after a variable delay T_2 a probe pulse with wave vector $\mathbf{k}_{pr}$ converts the propagated nuclear state into an optical signal that is emitted into the direction $\mathbf{k}_5=\mathbf{k}_{1''}-\mathbf{k}_{1'}+\mathbf{k}_{2''}-\mathbf{k}_{2'}+\mathbf{k}_{pr}$. (b) In the employed beam configuration the different third-order signals (crosses) are well separated from the desired fifth-order signal.

converts these motional states into an optical signal. Since two independent delay times are involved, information on the two-time correlation function is obtained. The central idea of this method is that in an inhomogeneously broadened (harmonic) ladder system, dephasing of a nuclear superposition state during T_1 might be nullified by rephasing of another superposition state during time T_2. This resembles the echo sequence of events, but in these fifth-order experiments rephasing and dephasing occur on different superposition states. Since rephasing during T_2 is only possible when there is memory of the preceding propagation during T_1, the occurrence of echo-type phenomena is indicative of the time scale(s) of the intermolecular dynamics.[22–24]

An extensive treatment of the theory of six-wave mixing was presented in Part I of this paper.[24] Using the Born–Oppenheimer approximation, a complete description of the nonresonant optical response up to fifth-order was given. In addition to the temporally two-dimensional part, discussed above, the fifth-order response comprises contributions due to processes involving instantaneous four- and six-wave mixing. These processes are not inherently two-dimensional and carry distinctly different dynamical information. Since they may interfere with the desired signal, they can complicate the interpretation of experimental results.

Attempts to measure the two-dimensional fifth-order response, and thereby characterize the nature of intermolecular motion for the first time by experiment, were recently reported by Tominaga and Yoshihara[25–28] and by ourselves.[29,30] Tominaga and Yoshihara observed for room temperature liquid carbondisulfide (CS_2) that the signal along the T_2-time coordinate depends only slightly on the value of T_1, which was varied from 0.5 to 1.5 ps. This result was interpreted in terms of the dynamics of two independent modes. A heavily overdamped mode accounts for the diffusive tails on a ps time scale, while a predominantly homogeneously broadened underdamped mode, with only a small static contribution to the line width, models the librations.[28] In our initial work, we did not observe a diffusive tail along the T_2 coordinate for CS_2 and benzene, but only ultrafast librational motion that damps out on a sub-ps time scale, independent of the particular value of T_1. The signal along the T_1 coordinate showed diffusive behavior and resembled at long delays the amplitude of the third-order signal.[29,30] Very recently, independent of the work presented here, Tokmakoff and Fleming performed similar experiments using a different beam geometry.[31] Their results agree in most aspects with those presented here.

Since our previous measurements suffered from an artefact due to mixing of the desired temporally two-dimensional fifth-order signal with a fifth-order local oscillator,[32] we present in this paper new results that we believe to be artefact free, because of a different phase matching configuration. The signals are now measured background free without the distortions by the temporal shape of the local oscillator and hence they can be evaluated much more accurately. The fifth-order signal shows a number of distinct features: The inertial librations determine the short time behavior of the fifth-order response along both time axes, but diffusion is only observed along the T_1 coordinate. The decay of the signal as a function of T_2 slows down when T_1 is increased from 0 to 500 fs. Then, it remains the same, irrespective of further increase of T_1. This behavior cannot be simulated by a model that projects librations and diffusion on two independent harmonic modes, using different degrees of inhomogeneous broadening for the librations. The model also fails to properly describe the difference in diffusive response along the two-time coordinates. The discrepancy between the calculations and the experiments is interpreted qualitatively in terms of a finite correlation time of the frequency fluctuations.

The paper is organized as follows: In Sec. II, experimental details are given. Section III discusses the four-wave mixing results. In Sec. IV, results of six-wave mixing experiments are assigned to a temporally two-dimensional Raman process. They are simulated in Sec. V in terms of the model used for the explanation of the four-wave mixing results. The shortcomings of this model are discussed. Finally, conclusions are formulated.

II. EXPERIMENT

The laser system, which has been described in detail elsewhere,[33] consists of a CPM laser and a copper vapor laser pumped amplifier. It produces 45 fs pulses at 620 nm with a pulse energy of 1.5 μJ. The third-order response of the liquid was measured using two techniques: the optically heterodyned detected optical Kerr effect (OHD-OKE) and transient grating scattering (TGS). For the OHD-OKE experiments, unamplified CPM pulses were used in a pump–probe configuration, as described by McMorrow and Lotshaw.[5]

Both TGS and two-dimensional six-wave mixing were performed with amplified laser pulses, using the beam con-

figuration shown in Fig. (1b). Initially, two coincident femtosecond pulses with wave vectors $\mathbf{k}_{1'}$ and $\mathbf{k}_{1''}$ induce a phase grating in the liquid. Then, after a variable delay T_1, a second pulse pair with wave vectors $\mathbf{k}_{2'}$ and $\mathbf{k}_{2''}$ again impulsively interacts with the sample. The third-order TGS signal was measured by blocking the second pulse pair, and detecting in the direction $\mathbf{k}_3=\mathbf{k}_{pr}+\mathbf{k}_{1''}-\mathbf{k}_{1'}$. The pump pulses $\mathbf{k}_{1'}$ and $\mathbf{k}_{2'}$ and the probe pulse $\mathbf{k}_{pr}$ were vertically polarized, while the pump pulses $\mathbf{k}_{1''}$ and $\mathbf{k}_{2''}$ were horizontally polarized. In centrosymmetric media this gives a horizontally polarized third-order signal.

The second pulse pair does not only form a grating, it also interacts with the molecules already excited by the first pulse pair. This gives rise to higher-order response. After a propagation period T_2, the probe pulse converts the resulting nuclear state into a six-wave mixing signal with wave vector $\mathbf{k}_5=\mathbf{k}_{pr}+\mathbf{k}_{2''}-\mathbf{k}_{2'}+\mathbf{k}_{1''}-\mathbf{k}_{1'}$. It is (nearly) phase matched, and clearly separated from third-order signals, as shown in Fig. 1(b).

The beam geometry was realized experimentally as follows: The probe pulse was split off from the incoming beam by a 1 mm thick uncoated fused silica plate and given a variable delay T_2 by a computer controlled delay stage. The remaining pulse was divided by a 50% beamsplitter, to generate the pulses for pulse pairs 1 and 2 with a variable delay T_1. Both of these beams were divided again by 50% beamsplitters to generate pulses $\mathbf{k}_{1'}$ and $\mathbf{k}_{1''}$ and pulses $\mathbf{k}_{2'}$ and $\mathbf{k}_{2''}$, respectively. The different path lengths were adjusted such that the pulses $\mathbf{k}_{1'}$ and $\mathbf{k}_{1''}$ arrived simultaneously at the sample, and $\mathbf{k}_{2'}$ and $\mathbf{k}_{2''}$ as well. All pulses were focused by a 250 mm fused silica singlet lens into a 2 mm fused silica cell. The angle between the beams of the first pulse pair was about 3.5°, while it was about 1.1° for the second pulse pair.

The total energy at the sample was kept below 300 nJ when a stationary sample was used, and below 600 nJ for a flowing sample. Both kind of samples gave identical results. No self-focusing or continuum generation was observed at these intensities. After the sample, the beams were recollimated by a 200 mm focal length lens, the signal was passed through a vertically orientated film polarizer and spatially filtered by a sequence of apertures and pinholes. It was detected by a photomultiplier tube and processed by a lock-in amplifier operating at the modulation frequency of the pulse $\mathbf{k}_{1''}$. CS_2 (Merck, p.a.) was used without further purification.

III. FOUR-WAVE MIXING

In this section we discuss the result of an optically heterodyned detected optical Kerr effect (OHD-OKE) experiment on CS_2 in order to illustrate the typical information content of a nonresonant four-wave mixing experiment. It will be demonstrated that the experiment can be modeled satisfactory for different degrees of inhomogeneity of the intermolecular vibrations.

In a time-resolved OHD-OKE experiment, an ultrashort pump pulse induces transient birefringence in an isotropic liquid by impulsive stimulated Raman scattering. The frequency range of excited motions is limited by the bandwidth

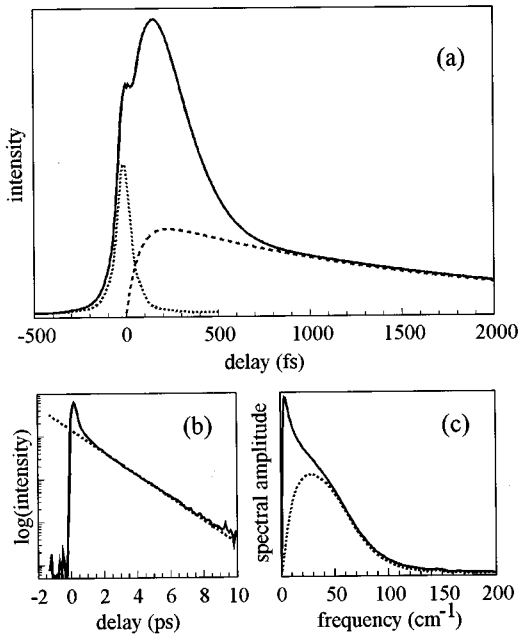

FIG. 2. (a) The OHD-OKE response of CS_2 (solid line). Three different contributions can be recognized: (i) Instantaneous response due to electronic hyperpolarizability, having the shape of the second-order autocorrelation of the pulses (short dashed line); (ii) Diffusive reorientation, modeled by an overdamped mode with exponential rise and decay times (long dashed lines); (iii) Coherent oscillations, dominating the short time (<1 ps) inertial response (remainder of the signal). (b) The diffusive tail of the signal is single exponential (dashed line) with a decay constant of 1.6 ± 0.1 ps. (c) Spectra of the nuclear response derived from the OHD-OKE data. The solid line gives the total spectrum of nuclear motion, while the dashed line is the spectrum of the coherent librations only.

of the laser pulse, which is in the order of a few hundred wave numbers for our 45 fs pulses. The build-up and decay of the birefringence is monitored by the polarization rotation of a variably delayed probe pulse.[4–6] For pump and probe pulses that are identical, except for a relative delay T, the third-order polarization can be written as

$$P^{(3)}(t,T)=E(t-T)\int_0^\infty d\tau_1 R^{(3)}(\tau_1)E^2(t-\tau_1). \tag{1}$$

Here, as in the remainder of the paper, the space indices of the polarization, the optical field, and the response function are suppressed for simplicity. Since the probe pulse also serves as an out-of-phase local oscillator, and the detector integrates the signal intensity over all times, the OHD-OKE signal varies with the pulse delay T as

$$I^{(3)}_{\mathrm{Kerr}}(T)=\int_{-\infty}^{\infty} dt\ \mathrm{Re}\{P^{(3)}(t,T)E(t-T)\}$$
$$=\mathrm{Re}\{G^{(2)}(T)\otimes R^{(3)}(T)\}, \tag{2}$$

where $G^{(2)}(T)$ is the second-order background-free intensity autocorrelation of the optical pulses and $\otimes$ denotes a convolution.

The result of an OHD-OKE experiment on room temperature liquid CS_2 is presented in Fig. 2(a). It agrees with previously published data of McMorrow *et al.*[4] The sharp

peak at zero delay is due to the instantaneous electronic hyperpolarizability of the liquid. This four-photon process is determined by the pulse duration and vanishes when the pump and probe pulse are separated in time. For finite delays, the signal is completely caused by the induced nuclear motion in the liquid. It reaches its maximum at a delay of 200 fs, reflecting the inertial character of this motion, and then rapidly decays in a nonexponential way. For delays longer than 2 ps the decay becomes single exponential, as can be seen in Fig. 2(b).

Useful insight in the intermolecular dynamics can be obtained by converting the time-domain nuclear response into the corresponding frequency-domain spectrum. Dividing this spectrum by the Fourier transform of the intensity autocorrelation gives a frequency representation of the true material response that is free of spectral filter effects caused by the finite duration/bandwidth of the laser pulses.[5] All information on the nuclear motion is, in principle, contained in the imaginary part of this complex ratio, which is shown as the solid line in Fig. 2(c).

The microscopic origin of the nuclear response is not completely clear. It is partly due to orientational motion of the individual CS_2 molecules, whose polarizability is highly anisotropic. However, the collective response from dimers, trimers, etc., that gives rise to pair correlations and interaction-induced changes of the polarizability, may also be important.[34–36] Up to now, there is no self-consistent and theoretical rigorous way to describe these many-body motions by closed-form expressions. It has been proposed to model these modes by a single harmonic coordinate with an effective frequency, damping parameter, and amplitude. However, this provides a sufficient number of fit parameters, rather than any physical insight, as already pointed out by Frenkel and McTague.[34] In order to avoid the ambiguities of unwarranted assumptions about these motions, Ruhman and Nelson[37] proposed to treat only single-molecule motion explicitly, and to discuss the possible shortcomings of this model in the light of possible many-body effects. Since very little is known, yet, about interaction-induced effects and many-body contributions in higher-order nonlinear experiments, we follow this strategy as well, and try to model our third- and fifth-order results by single-molecule orientational motion only. This is not motivated by the relative importance of the distinct contributions, but rather by the complexity of treating the full problem.

The single-molecule orientational motion, as observed in the OHD-OKE experiment, can be described qualitatively as follows: Initially, the molecules are excited by impulsive stimulated Raman scattering, and start to librate in phase in the potential wells, formed by the neighbor molecules. This coherent motion may decay by loss of the phase relations between the excited molecules due to pure dephasing or inhomogeneous line broadening, or by dissipative damping of the individual motions. After this decay, the originally isotropic situation is not restored, because the excited molecules have perturbed their surroundings, leading to a net orientation. This orientation, which involves the displacement of many molecules, finally decays by diffusion.

In a widely used phenomenological model the coherent librations (L) and the diffusion (D) are treated as independent harmonic modes. The third-order response function is then given by

$$R^{(3)}(\tau_1)=c_L^{(3)}R_L^{(3)}(\tau_1)+c_D^{(3)}R_D^{(3)}(\tau_1). \tag{3}$$

Here, $R_L^{(3)}$ and $R_D^{(3)}$ are the third-order response functions of the harmonic oscillators, while the constants $c_L^{(3)}$ and $c_D^{(3)}$ parametrize the coupling of the two modes in third-order response with the light fields.

Since the diffusive decay is slow compared to the motions of individual molecules, the influence of these microscopic motions is averaged out. Therefore, we model it by a purely homogeneously broadened oscillator.[28,30] There has been quite a debate in the literature about the relaxation characteristics of the librational motion, which has been modeled by one, two, or a continuous distribution of underdamped, overdamped, or critically damped harmonic modes, which may be homogeneously or inhomogeneously broadened.[4–8,37,38] In order to treat the modes in both the underdamped ($\gamma/2<\omega$) and overdamped ($\gamma/2>\omega$) limit, and to allow a continuous change between them, we follow Tanimura and Mukamel.[22] They introduced damping by coupling the modes linearly to a set of Brownian oscillators, which leads to level-independent population relaxation characterized by a rate γ. In the lowest order of the expansion of the electronic polarizability in the nuclear coordinate, the underdamped third-order response function is[22,24]

$$R_{\mathrm{UN}}^{(3)}(\tau_1)=e^{-(\gamma/2)\tau_1}\frac{1}{\Omega_{\mathrm{UN}}}\sin(\Omega_{\mathrm{UN}}\tau_1), \tag{4}$$

where $\Omega_{\mathrm{UN}}=(\omega^2-\gamma^2/4)^{1/2}$ is the reduced frequency of the mode. The corresponding response function of the overdamped oscillator is[22,24]

$$\begin{aligned}R_{\mathrm{OV}}^{(3)}(\tau_1)&=e^{-\gamma/2\tau_1}\frac{1}{\Omega_{\mathrm{OV}}}\sinh(\Omega_{\mathrm{OV}}\tau_1)\\&=\frac{1}{2\Omega_{\mathrm{OV}}}(1-e^{-\tau_1/\tau_R})e^{-\tau_1/\tau_D},\end{aligned} \tag{5}$$

with $\Omega_{\mathrm{OV}}=(\gamma^2/4-\omega^2)^{1/2}$.

Different models for the damping, which were presented in Part I of this paper,[24] rely on the weak coupling limit and cannot be applied to strongly damped oscillators. The last expression of Eq. (5) is equal to that used by McMorrow and Lotshaw,[38] who employed the exponential decay and rise times τ_D and τ_R as fitting parameters. These are related to the frequency and the damping rate of the overdamped oscillator by: $1/\tau_D=\gamma/2-\Omega_{\mathrm{OV}}$ and $1/\tau_R=2\Omega_{\mathrm{OV}}$. The decay time of the heavily overdamped diffusive mode, $\tau_D=1.65$ ps, can be accurately determined from the experiment, as shown in Fig. 2(b). The rise time τ_R is not as easily extracted. McMorrow and Lotshaw[38] pointed out that the particular value of τ_R has only a minor influence on the low energy side of the nuclear spectrum. It was set to $\tau_R=0.121$ ps in our fitting procedure.

For pure homogeneous broadening of the librations, the dynamic parameters found are: $\gamma_L=14.79$ ps^{-1} and $\omega_L=8.24$ rad ps^{-1}. This means that the librational mode, modeled by

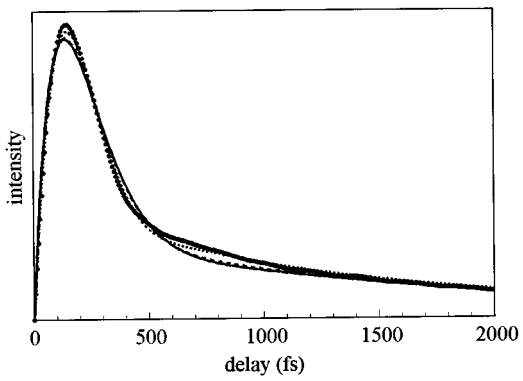

FIG. 3. Fit of the deconvoluted nuclear response obtained from OHD-OKE experiment (dots) to two harmonic modes, one heavily overdamped modeling the diffusion and one nearly critically damped describing the coherent librations. The later is modeled in the homogeneous limit (solid line) and for two degrees of inhomogeneity $\sigma=1.00$ rad ps^{-1} (long dashed line) and $\sigma=2.53$ rad ps^{-1} (short dashed line). The parameters of the fit are given in the text.

the underdamped oscillator Eq. (4), is nearly critically damped ($\gamma_L/2\approx\omega_L$). The fit is shown together with the deconvoluted nuclear response function in Fig. 3. The values of γ_L and ω_L can be changed within approximately 10% without a significant change in the quality of the fit. The ratio of the amplitudes of the librational and diffusive mode is 7.3.

The spectrum of the librational mode, which was obtained by subtracting the diffusive response from the experimental data prior to the Fourier deconvolution, is shown as the dashed line in Fig. 2(c). When a static distribution of local potentials, and hence of oscillator frequencies, contributes to this spectrum, the part of the nonlinear response function that is due to the librational motion has to be integrated over this distribution:

$$R_L^{(3)}(\tau_1)=\int_0^\infty d\omega g(\omega)R_L^{(3)}(\omega,\tau_1), \tag{6}$$

where $g(\omega)$ is the frequency distribution function. $R_L^{(3)}(\omega,\tau_1)$ is now given by Eq. (4) or Eq. (5), depending on the limit that applies. In the pure inhomogeneous limit, the exponential damping rate γ_L can be neglected and hence no renormalization of the oscillator frequency occurs. The distribution function $g(\omega)$ is then simply equal to the spectrum of Fig. 2(c), multiplied by ω. Since this spectrum is calculated in a model-independent way by Fourier transforming the data, Eq. (6) with this distribution function reproduces the data perfectly.

When the response is modeled for both homogeneous and inhomogeneous broadening of the librational motion, a functional form of the distribution function $g(\omega)$ has to be assumed. Ruhman and Nelson used a modified Gaussian distribution for this purpose:[37]

$$g(\omega)=\omega\ \exp\left\{-\frac{(\omega-\omega_L)^2}{2\sigma^2}\right\}, \tag{7}$$

where σ is the width of the distribution. Equation (6) is suitable to describe the continuous change from underdamped to overdamped oscillators within the inhomogeneous distribution. In Table I, values for ω_L, σ, and γ_L are shown, obtained from fitting the deconvoluted OKE response to Eq. (3) with partly inhomogeneously broadened librations, described by Eq. (6), and diffusion, modeled by Eq. (5). The values for ω_D and γ_D were always 2.32 rad ps^{-1} and 9.5 ps^{-1}, respectively. The best fit to the data is obtained for $\sigma=2.52$ rad ps^{-1}, but all fits with some inhomogeneity are still better than the one in the homogeneous limit; see Fig. 3.

TABLE I. Parameter sets for the librational motion, obtained from fitting the deconvoluted OKE response. γ_L is the homogeneous (exponential) damping rate, ω_L is the central librational frequency, and σ is the width of the inhomogeneous distribution of librational frequencies, which has the modified Gaussian form of Eq. (7).

γ_L/ps^{-1}	14.79	13.85	10.14
ω_L/rad ps^{-1}	8.24	8.16	7.62
σ/rad ps^{-1}	⋯	1.00	2.53

Thus, the coherent librational motion can be modeled satisfactory in the limits of homogeneous and inhomogeneous broadening, or both. This demonstrates that the third-order experiment cannot discriminate between the various possibilities, since all can be made to fit the experimental results fairly well.

IV. SIX-WAVE MIXING

In this section, the results of six-wave mixing experiments on CS_2 are presented. The purpose of extending the four-wave mixing experiments to higher-order nonlinear response is to obtain information on the time scale of the intermolecular dynamics through multi-time correlation functions.[22–30] Hence, two or more delay times should be involved. Since higher-order experiments are quite complex, a variety of artifacts can disturb the signals. Before interpreting the results in terms of the nuclear dynamics in Sec. V, we carefully characterize the observed signals in order to unambiguously assign them to the desired temporally two-dimensional fifth-order process.

For identical optical pulses, given the appropriate delays T_1 and T_2, the fifth-order polarization can be written as

$$P^{(5)}(t,T_1,T_2)=E(t-T_1-T_2)\int_0^\infty d\tau_1\int_0^\infty d\tau_2\ R^{(5)}(\tau_1,\tau_2)\times E^2(t-T_1-\tau_2)E^2(t-\tau_1-\tau_2). \tag{8}$$

Ideally, the fifth-order signal, which is integrated by the detector, is emitted in a direction where there are no other fields present. Its delay dependence is then given by

$$I_5(T_1,T_2)=\int_{-\infty}^\infty dt|P^{(5)}(t,T_1,T_2)|^2. \tag{9}$$

The theory of the fifth-order nonlinear optical response is extensively discussed in Part I of this paper.[24] In general, the fifth-order response function $R^{(5)}(\tau_1,\tau_2)$ consists of several contributions which provide different dynamical information. In Fig. 4 the various processes are shown in an energy

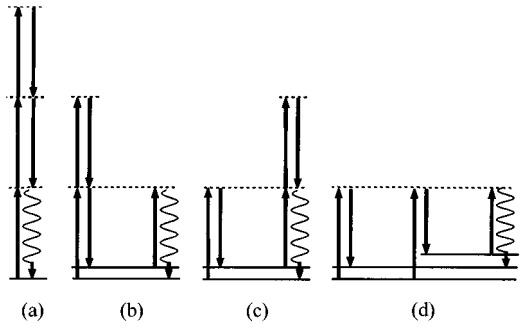

FIG. 4. The four different processes that can contribute to six-wave mixing: (a) Purely electronic fifth-order polarization is instantaneous. (b) Hyper-Raman scattering followed by an ordinary Raman process cannot contribute to the fifth-order response for finite delay T_1. (c) Raman scattering followed by a four-photon hyper-Raman interaction can contribute to the fifth-order response only when the probe pulse overlaps with the second pulse pair. (d) Three subsequent Raman scattering events give rise to a two-dimensional Raman process.

level diagram. Process (a) is due to a higher-order electronic hyperpolarizability and contains no information on the intermolecular dynamics. Processes (b) and (c) depend on a single delay time, and contain information similar to that of conventional four-wave mixing. The temporally two-dimensional process (d) is the source of additional dynamic information, not available from lower-order experiments. It consists of three consecutive Raman scattering processes, that are separated by the variable delays T_1 and T_2. It was this term that was discussed in the key paper of Tanimura and Mukamel on this subject.[22]

In Fig. 5, the results of fifth-order experiments are shown along the two time coordinates T_2 and T_1. The third-order transient grating scattering (TGS) signal, which is related to the OHD-OKE experiment and determined by the absolute square of the third-order polarization, is also displayed. Before we discuss these results in detail, it is important to establish that indeed two-dimensional fifth-order signals were observed. The observations that support this assignment are: (i) The signal is emitted in the expected direction $\mathbf{k}_5=\mathbf{k}_{1''}-\mathbf{k}_{1'}+\mathbf{k}_{2''}-\mathbf{k}_{2'}+\mathbf{k}_{\mathrm{pr}}$. It is not observed in other directions; (ii) The signal vanishes when any of the five incoming pulses is blocked; (iii) The signal depends on the fifth power of the applied laser pulse intensity; this is shown in Fig. 6; (iv) The signal has the expected vertical polarization. It disappears when the analyzer is oriented horizontally.

These arguments do not exclude the possibility that a sequence of lower-order processes contributes to the signal.[28,39–41] These are emitted in the same direction and have the same power dependence as the fifth-order signal. In our case, the most important of these processes involves the sequence of two third-order processes: The pulse $\mathbf{k}_{2''}$ is scattered off a grating, produced by pulses $\mathbf{k}_{1'}$ and $\mathbf{k}_{1''}$. The generated intermediate field $\mathbf{k}_i=\mathbf{k}_{1''}-\mathbf{k}_{1'}+\mathbf{k}_{2''}$ forms together with pulse $\mathbf{k}_{2'}$ a second grating which scatters the probe pulse $\mathbf{k}_{\mathrm{pr}}$ in the direction $\mathbf{k}_5=\mathbf{k}_i-\mathbf{k}_{2'}+\mathbf{k}_{\mathrm{pr}}$. To minimize the efficiency of this sequence of events, the beam configuration was chosen such that the intermediate third-order amplitude

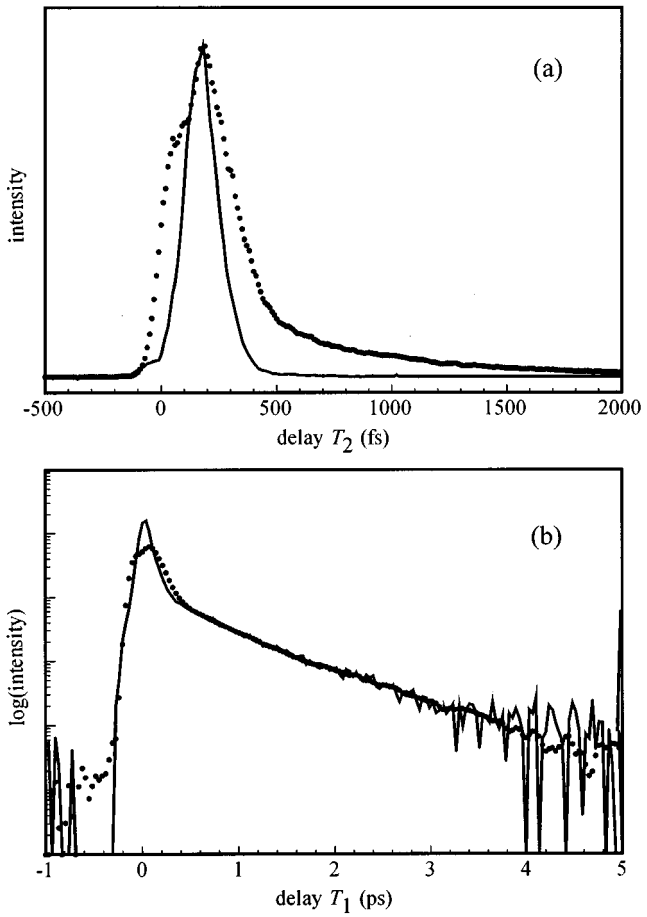

FIG. 5. (a) Third-order grating scattering signal (dots) and fifth-order signal as function of the probe delay T_2 (shown for $T_1=0$ by the solid line). The latter does not possess a significant instantaneous contribution and shows an inertial rise time comparable to that of the third-order grating signal. It is free of any diffusive tail. (b) Third-order grating scattering signal (dots) and fifth-order signal as function of the delay T_1 (shown for $T_2=170$ fs by the solid line). For large delays T_1 both decay exponentially with a time constant of 800 fs. The maximum of the signal at short delay is about a factor of 3 stronger for the fifth-order signal than for the grating scattering experiment, when both are scaled on the exponential tail.

is badly phase mismatched. The sample was thick enough to accomplish this. For this sequential process, the same dynamics as in ordinary third-order grating scattering is expected along both time axes, T_1 and T_2. Since the fifth-order response of Fig. 5(a) is free from any diffusive tail within the experimental accuracy, it can be concluded that sequential processes do not contribute to either of the traces of Fig. 5.

The six-wave mixing signals of Fig. 5 can be assigned unambiguously to the fifth-order process of Fig. 4(d): It is clear from Fig. 5(a), where the T_2 dependence is shown for $T_1=0$, that there is hardly any signal at $T_2=0$, where all pulses temporally overlap. This indicates that the contribution from the process of Fig. 4(a) is negligible. The process, depicted in Fig. 4(b), involves an instantaneous four-photon interaction, governed by the coordinate dependent electronic hyperpolarizability. It is only possible when both pulse pairs overlap. Since no pulsewidth limited transient is observed at $T_1=0$ in Fig. 5(b), and the shape and intensity of the

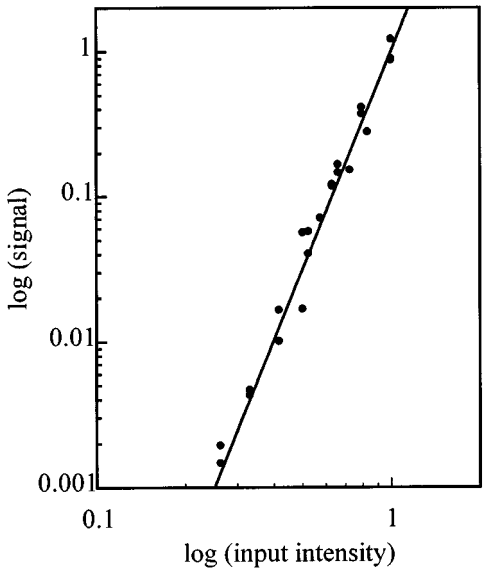

FIG. 6. Intensity dependence of the observed six-wave mixing signals (dots). The intensity of all five excitation pulses was changed simultaneously in this experiment. The solid line shows the theoretical fifth-order dependence on the overall power.

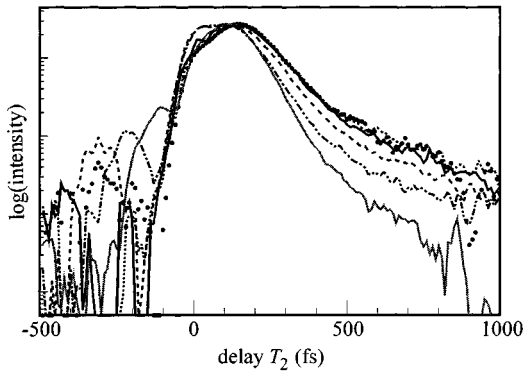

FIG. 7. Fifth-order signals as function of the probe delay T_2 for different values of the delay T_1. This value of T_1 increases from bottom to top according to the following indications for the lines: 100 fs (gray), 200 fs (dashed-dotted), 300 fs (long dashed), 400 fs (solid), 500 fs (dotted), and 1000 fs (short-dashed). The decay time of the tail of the signal increases from ca. 130 fs for $T_1=100$ fs to ca. 250 fs for $T_1=500$ fs. Further increase of T_1 has no effect on the signal shape. Along the T_2 coordinate, no trace of a diffusive decay with a time constant of 800 fs can be found.

T_2-dependent signal changes smoothly when T_1 is increased from 0 to 100 fs (*vide infra*), it can be concluded that the contribution of the process of Fig. 4(b) is of minor importance in our data. The process of Fig. 4(c), which also contains a four-photon interaction, can only contribute when the probe pulse coincides with the second pulse pair. This may lead to a pulsewidth limited signal at $T_2=0$. Again, it can be concluded from the data that this contribution can be ignored in our data analysis. The conclusion therefore is that the processes 4(a)–4(c) are all negligible compared to that of Fig. 4(d). The fifth-order response is completely determined by this temporally two-dimensional process.

We now briefly return to a recently published paper,[30] in which we reported results of six-wave mixing experiments on room temperature liquid CS_2 and benzene. In that geometry the pulse pairs were aligned interferometrically, so that the signal could not be measured for small delays T_1. The major difference with the results, presented here, concerns the exponential decay along the T_1 coordinate. After a fast nonexponential part, the earlier reported signal resembled the amplitude of the TGS experiment instead of the intensity. We have now established that in the original beam geometry an additional, previously ignored fifth-order signal from second-order Bragg diffraction is present, that acts as a local oscillator.[32]

V. FIFTH-ORDER DYNAMICS

In this section we analyze the results of the femtosecond six-wave mixing experiments in terms of the model used in Sec. III for the four-wave mixing data. The signal along the T_2 coordinate, shown in Fig. 5(a) for $T_1=0$ fs, resembles the inertial, librational part of the third-order response, while no diffusion is observed. The maximum occurs at about 170 fs, which is slightly faster than the four-wave mixing maximum.[42] In Fig. 7, the T_2 dependence of the six-wave mixing signal for different values of T_1 is shown. The overall shape and position of the signal change when T_1 is increased from 100 to 500 fs, but it remains unaffected when T_1 is enlarged further. The maximum of the signal slightly shifts toward larger values (from 120 to 150 fs) when T_1 is varied between 100 and 500 fs, but no clear echo behavior is observed. The signal shape becomes broader, and the decay of the tail slows down from 130 fs to 250 fs, when fitted to a single exponential. These features were not reported by Tominaga and Yoshihara,[25–28] who obtained data only for larger delays T_1, nor by Tokmakoff and Fleming,[31] who probed different tensor elements with slightly longer pulses.

The T_1 dependence of the signal, shown in Fig. 5(b) for $T_2=170$ fs, peaks close to zero delay, where the two pulse pairs overlap. For T_1 values between 0 and -170 fs, the ''first'' pulse pairs arrives between the ''second'' pulse pair and the probe, so that both T_1 and T_2 change in a diagonal delay scan. For delay T_1 positive, the fast nonexponential decay becomes single exponential at longer delays, with the same time constant $\tau_D=800$ fs as in the TGS signal. The maximum of the six-wave mixing signal is about a factor of 3 larger than that of the TGS signal, when scaled on the diffusive tail. Both the coherent librations and the diffusion of the third-order response determine the fifth-order signal along the T_1 coordinate.

In order to test the dynamic model of the third-order response, based on the description of librations and diffusion by two independent harmonic modes, we extend it to yield a fifth-order response function that can then be written as:[24]

$$R^{(5)}(\tau_1,\tau_2)=c_L^{(5)}R_L^{(5)}(\tau_1,\tau_2)+c_D^{(5)}R_D^{(5)}(\tau_1,\tau_2). \qquad (10)$$

The relative magnitude of the coupling constants $c_L^{(5)}$ and $c_D^{(5)}$ will, in general, be different from that of the third-order response, since these constants are determined by different orders of the expansion of the electronic polarizability in the

relevant nuclear coordinate.[24] The expansion coefficients cannot be predicted as long as the nature of these modes is not completely clear. When a number of independent modes is invoked to model the material response in third order, this leads to a quite complicated situation in fifth order. For instance, a particular mode that dominates the third-order signal may yield a negligible contribution to the fifth-order response. Lacking further knowledge about the amplitude of each mode, they have to be determined from the fifth-order experiment.

When the polarizability is expanded up to second order in the harmonic coordinate q, this yields a finite fifth-order response. Assuming level-independent population relaxation as the only damping mechanism and considering only terms in lowest order of q, the fifth-order response function can be evaluated for under- ($\gamma/2<\omega$) and overdamped ($\gamma/2>\omega$) harmonic motion by the theory of Tanimura and Mukamel:[22,24]

$$\begin{aligned} R_{\mathrm{UN}}^{(5)}(\tau_1,\tau_2) = e^{-\gamma/2(\tau_1+\tau_2)}\,\frac{1}{\Omega_{\mathrm{UN}}^2}\,[&\cos\,\Omega_{\mathrm{UN}}(\tau_1-\tau_2) \\ &-\cos\,\Omega_{\mathrm{UN}}(\tau_1+\tau_2)] \\ &+e^{-\gamma/2(\tau_1+2\tau_2)}\,\frac{1}{\Omega_{\mathrm{UN}}^2}\,[\cos\,\Omega_{\mathrm{UN}}\tau_1 \\ &-\cos\,\Omega_{\mathrm{UN}}(\tau_1+2\tau_2)], \end{aligned} \tag{11}$$

$$\begin{aligned} R_{\mathrm{OV}}^{(5)}(\tau_1,\tau_2) = e^{-\gamma/2(\tau_1+\tau_2)}\,\frac{1}{\Omega_{\mathrm{OV}}^2}\,[&\cosh\,\Omega_{\mathrm{OV}}(\tau_1-\tau_2) \\ &-\cosh\,\Omega_{\mathrm{OV}}(\tau_1+\tau_2)] \\ &+e^{-\gamma/2(\tau_1+2\tau_2)}\,\frac{1}{\Omega_{\mathrm{OV}}^2}\,[\cosh\,\Omega_{\mathrm{OV}}\tau_1 \\ &-\cosh\,\Omega_{\mathrm{OV}}(\tau_1+2\tau_2)], \end{aligned} \tag{12}$$

where again $\Omega_{\mathrm{UN}}=(\omega^2-\gamma^2/4)^{1/2}$ and $\Omega_{\mathrm{OV}}=(\gamma^2/4-\omega^2)^{1/2}$.

For an inhomogeneous distribution of librational frequencies, the fifth-order response function has to be integrated over this distribution, similar to the third-order response:

$$R_L^{(5)}(\tau_1,\tau_2)=\int_0^\infty d\omega\, g(\omega) R_L^{(5)}(\omega,\tau_1,\tau_2). \tag{13}$$

This form again allows for a continuous change from an underdamped to an overdamped oscillator. The response function $R_L^{(5)}(\omega,\tau_1,\tau_2)$ is given by Eq. (11) or Eq. (12), depending on the particular values of ω and γ. The distribution $g(\omega)$ enhances the decay of most terms of Eqs. (11) and (12), due to the fact that many cosine functions beat against each other. This does not hold for the $\cos\,\Omega_{\mathrm{UN}}(\tau_1-\tau_2)$ part, which describes a possible recurrence of macroscopic nuclear coherence in the inhomogeneous limit.[23,24,28] This works as follows: Pulses $\mathbf{k}_{1'}$ and $\mathbf{k}_{1''}$ generate a one-quantum superposition state, e.g., $|\lambda\rangle\langle\lambda\pm1|$, which dephases during propagation time τ_1. Here, λ designates the motional quantum number. Then, the second pulse pair $\mathbf{k}_{2'}$ and $\mathbf{k}_{2''}$ induces a two-quantum transition, so that a superposition state is created with a phase factor that has the opposite sign. This state could, for instance, be $|\lambda\rangle\langle\lambda\mp1|$. Then the phases acquired during propagation times τ_1 and τ_2 compensate for each other when $\tau_1=\tau_2$, independent of the particular frequency ω of the oscillator. This leads to a motional echo. In the other extreme case of pure homogeneous broadening, rephasing is impossible, since the loss of macroscopic coherence is then irreversible.

The unique information content of the temporally two-dimensional fifth-order experiment was demonstrated in Part I of this paper by model calculations for the spectral response of the libration in CS_2.[24] In the inhomogeneous limit, the calculated signal indeed always reaches its maximum at $\tau_1=\tau_2$. After an initial decay due to nonrephasing pathways, the signal intensity at the maximum stays the same: an echo is formed that does not decay for a purely static distribution of frequencies. In the homogeneous limit, the signal always peaks directly after the second pulse pair. Its shape and position do not change when τ_1 is varied. The magnitude of the signal decreases monotonically because of irreversible loss of coherence.

The data of Fig. 7 do not exhibit a clear echo-type response at $T_2=T_1$ but they are not identical either. In order to investigate the possible role of a finite inhomogeneous contribution to the librational line shape, we calculated the fifth-order response of the librational mode for different inhomogeneous widths, using Eq. (13). The parameters and the functional form for $g(\omega)$ were the same as those obtained from the fits of the third-order response and are displayed in Table I. The results for the calculated fifth-order intensity along the T_2 coordinate are shown in Fig. 8. For simplicity, delta-function shaped pulses were assumed in the calculations. The agreement between the measured response and the calculations is best for a value of $\sigma\approx1.0$ rad ps^{-1}, which corresponds to a distribution with a width that is about 25% of the center frequency ω_L. However, the inclusion of a static inhomogeneity does not explain that the measured T_2 traces for $T_1=0.5$ ps and 1.0 ps have the same shape. Static inhomogeneity will always lead to a monotonic lengthening of the decay when T_1 is increased. Moreover, none of the calculations can account correctly for the relatively slow tails at T_2 bigger than 0.5 ps in Fig. 7.

Before we discuss possible reasons for this discrepancy, we focus on the role of diffusion that has been completely neglected in the calculations of Fig. 8. An important feature of the present formulation of the optical dynamics in terms of two independent modes is that the least-damped oscillator will always dominate the signal when T_1 and/or T_2 is much larger than the homogeneous relaxation time of the heavily damped mode.[24] Based on the third-order experiment, where we found $\tau_D\approx10\tau_L$ for the relaxation times of the diffusion and the libration, it is expected that the diffusion dominates the signal when T_1 or T_2 is large.

The T_1 dependence of the fifth-order signal, displayed in Fig. 5(b) for a delay $T_2=170$ fs, shows a distinct exponential decay with the same decay time of 800 fs as observed for the diffusion in the third-order TGS experiment. Since the ratio of the librational and diffusive contribution to the fifth-order

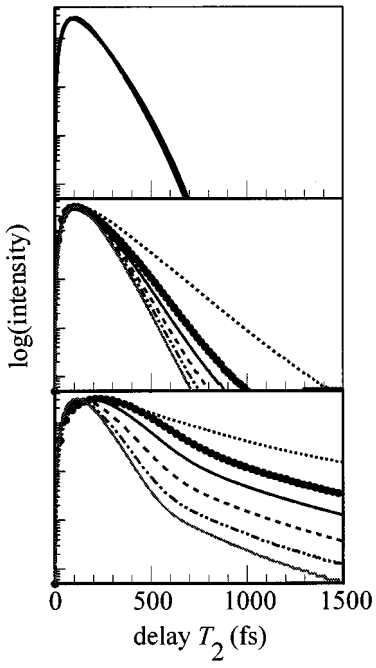

FIG. 8. Calculated fifth-order signals of the librations in liquid CS_2 along the time delay T_2. Different degrees of inhomogeneities were assumed: $\sigma=0$ rad ps^{-1} (top panel), $\sigma=1.0$ rad ps^{-1} (middle panel) and $\sigma=2.53$ rad ps^{-1} (bottom panel). The different lines indicate different values for the time delay T_1: 100 fs (gray), 200 fs (dashed-dotted), 300 fs (long dashed), 400 fs (black), 500 fs (dotted), and 1000 fs (short-dashed). The used sets of parameters for γ_L, ω_L, and σ are obtained from fitting the third-order response (see Table I). The curves have been rescaled to the same height. In the homogeneous limit (top), the fifth-order signal does not change its shape. It shows always the same rise time followed by a fast decay. With an inhomogeneity of 20% of the center frequency (middle), the decay slows down and increases slightly with increasing T_1. This feature becomes more pronounced when the inhomogeneity is further increased (bottom).

intensity along T_1 is a factor of 3 larger than that in the third-order experiment, where we found $c_L^{(3)}/c_D^{(3)}\approx 7.3$, we estimate that the ratio of the amplitudes $c_L^{(5)}/c_D^{(5)}$ is approximately 10. However, the fifth-order signal along T_2, displayed in Fig. 7, does not show any diffusion even for the largest value of $T_1=1.0$ ps. The observed decay times, ranging from 130 to 250 fs, are more than a factor of 3 smaller than that of the diffusion. The expressions for the fifth-order response in Eqs. (11) and (12) are not symmetric in τ_1 and τ_2: Along τ_1 all terms decay with a single decay constant γ, while the decay along τ_2 is double exponential with decay constants γ and 2γ. It is clear that the discrepancy of the decay times cannot be explained in this way. Hence, the amplitude of the diffusion is much smaller than that of the libration in fifth order. Based on the T_2 dependence, we estimate that the amplitude $c_D^{(5)}$ is at least three orders of magnitude smaller than the amplitude of the librations $c_L^{(5)}$. It must be concluded that the two estimates for the ratio of $c_L^{(5)}$ and $c_D^{(5)}$ along the two time coordinates are in clear contradiction with each other. Diffusion is prominently present along one time variable while it is completely absent along the other. A similar observation was made by Tokmakoff and Fleming[31] who reported diffusive behavior along T_1 but no sign of a slow decay along T_2. Tominaga and Yoshihara[25–28] did not show any traces along T_1 in their papers.

Based on the experimental results and the model calculations we can conclude that the simple model, introduced in Sec. (III), fails dramatically to explain the full temporally two-dimensional information content of the fifth-order experiment. The entirely different behavior along the two different axes cannot be understood at all by the employed model with two independent modes. The second experimental feature that cannot be covered even qualitatively by the model concerns the change of the signal shape along T_2, when T_1 is increased from 100 to 500 fs, while it is unaffected by a further enlargement. Because the signals were carefully assigned to a temporally two-dimensional Raman process, we believe that the discrepancies between the experiment and the theory are a signature of the failure of the employed model to properly describe liquid state dynamics.

To conclude this section we review the invoked simplifying assumptions of the theory and discuss possible future improvement in the light of the available experimental data. Modeling libration and diffusion as two independent modes [see Eqs. (3) and (10)] may be related to the failure in explaining the different dynamical behavior along the two time axes. In a more realistic description these modes should be coupled, as can be clearly seen from the following phenomenological description: The initially excited single-molecule librational motion occurs in potential wells, which define its equilibrium position and libration frequency. This motion, however, causes substantial distortions of the local structure and results in a new equilibrium position and a macroscopic anisotropy. On a longer time scale the thermal motion of the surrounding molecules causes the decay of this orientational anisotropy by diffusion. A theory that is close to this picture of liquid state dynamics is the itinerant oscillator model,[43–45] which was initially developed for the explanation of FIR absorption data. In this model, the optical field(s) induce motions of an optically active oscillator which is coupled to an overdamped collective mode, modeling the many-body (diffusive) dynamics of the surrounding molecules. Recently, Ruhman and Nelson generated correlation functions from their third-order TGS data and analyzed them, using some simplifications, by this theory.[37] It seems promising to extend this model to generate higher-order nonlinear optical response functions.

Within the general picture of this model the separation of the dephasing processes into homogeneous and inhomogeneous becomes quite dubious. The change of the local potential on excitation will lead to a finite correlation time of the initial inhomogeneous frequency distribution. In such a situation the dynamics are expected to exhibit a distinct non-Markovain character, reflecting the finite memory times of the system. When investigated by conventional echo techniques, the non-Markovian dynamics gives rise to a well-known feature: When the propagation times are increased, the echo profile initially changes, but stays the same when they exceed the memory time of the system.[46] We have observed that the T_2 trace does not depend on T_1 when that

delay is larger than 0.5 ps. This gives strong indications that the intermolecular potential fluctuations possess a finite memory time that is in the order of 500 fs. An improved model of the liquid state dynamics should account for this effect.

Another approach to improve the existing theory might be to refine the description of the relaxation processes. Traditionally vibrational dephasing and relaxation are separated into T_1 and T_2 processes describing population relaxation and pure dephasing which may explicitly depend on the involved vibrational levels. The employed model of Tanimura and Mukamel,[22] which is to our knowledge the only model applicable to strongly damped systems, describes only level-independent population relaxation. An extension of this model to include pure dephasing and level-dependent relaxation is highly nontrivial since it requires the treatment of nonlinear system-bath coupling and an anharmonic bath by path integral techniques. Also, it is not clear whether this will lead to an understanding of the finite correlation time of the frequency fluctuations, and of the unclear interplay between diffusion and libration.

The used model that relies on the explicit description of two harmonic modes only, may be extended by including more independent modes. Tokmakoff and Fleming,[31] who have invoked up to 20 modes in their simulations of the fifth-order response of CS_2, demonstrated that this does not overcome the problems in modeling the experimental results. They assumed that the third- and fifth-order amplitudes were identical. Instead of introducing more modes, it is also possible to modify the character of the nuclear motion. In the model of Tanimura and Mukamel[22] the nonlinearity of the probed nuclear motion is introduced by a nonlinear dependence of the polarizability on the nuclear coordinate. In the first experimental paper on nonlinear Raman scattering, Lukasik and Ducuing[39] already pointed out that nonlinearity can also be introduced by assuming an anharmonic potential for the nuclear motion. Very recently, Okumura and Tanimura[47] have calculated the fifth-order response for this case, using perturbation theory. They concluded that the anharmonicity in CS_2 is relatively small compared to the nonlinear coordinate dependence of the polarizability.

The explicit inclusion of many-body effects, such as pair correlations and interaction-induced effects,[34–36] may also help to improve the quality of the simulations. Unfortunally, the role of these effects is not fully understood even in third-order nonlinear experiments. No theoretical description of these many-body effects in a nonlinear optical perturbation treatment has been reported yet. This is mainly due to the complexity of the problem, which involves the mutual orientations and distances of several molecules, averaged over the liquid. Future progress in the understanding of these effects will therefore depend on systematic experimental investigations and molecular dynamics simulations.[36] Up to now only one fifth-order experiment on binary mixtures has been reported.[27] It is clear from this discussion that further experimental and theoretical efforts have to be made to improve our understanding of the rich dynamics of liquids.

VI. CONCLUSIONS

Results of nonresonant femtosecond four- and six-wave mixing experiments on neat CS_2 were reported. The intermolecular structure and dynamics cannot be characterized uniquely by third-order experiments, like optical Kerr effect and transient grating scattering. The results for room temperature CS_2 show that the response at short times is dominated by coherent librations, which are nearly critically damped and can be adequately described with different degrees of inhomogeneity. At longer delays the dynamics are due to slow diffusive reorientation.

The time-domain fifth-order response, probed along two independent propagation times, is, in principle, sensitive to the dephasing mechanisms. For an inhomogeneous distribution of frequencies, rephasing of the nuclear motion can be induced, leading to a motional echo when the two propagation times are equal. In the limit of homogeneous broadening the loss of coherence is irreversible, and hence no echo behavior is observed. None of the two limit cases was found in the observed fifth-order signal, which was assigned to three subsequent Raman scattering events. Processes involving higher-order hyperpolarizabilities and sequential third-order processes do not yield a significant contribution to the observed signals.

The fifth-order signal as function of the second delay time, which seems to be governed by librations only, changes when the first delay time is increased up to 500 fs, but remains unchanged when that delay is enlarged further. The maximum slightly shifts toward larger delays and the tails substantially slow down when the first propagation time is getting longer, but no clear echo behavior is observed. When the first delay time is varied, for a fixed second delay time, the observed transient exhibits both a librational contribution at short times and a diffusive component on a ps time scale. In fifth order the relative contribution of the diffusive component is about a factor of 3 smaller than in third-order response, though.

The results of the four- and six-wave mixing experiments were interpreted in a phenomenological model, which treats the libration and diffusion as two independent harmonic modes. The third-order optical Kerr effect results can be simulated satisfactory for different amounts of inhomogeneous broadening of the librations. When extended to fifth order, this model accounts for some of the experimental features. It fails to explain why diffusion is present along the first time coordinate, while it is completely absent along the second. Using just a weakly inhomogeneously broadened underdamped oscillator and no diffusive mode, the data along the second propagation time can be understood only qualitatively. In particular, the model cannot account for the fact that the traces are independent of the first delay time when that exceeds 500 fs.

This peculiar feature is typical for systems that exhibit non-Markovian dynamics due to a finite correlation time of the frequency fluctuations. Several ways to overcome the problems related to the assumptions of the model were discussed. It seems promising to extend the itinerant oscillator

model to higher-order nonlinear optical experiments since it is in principle capable to mimic both the coupling of libration and diffusion and the finite correlation time of the dynamic distribution of librator frequencies. The theory may be improved further by allowing for level-dependent relaxation rates for energy and phase relaxation and by including anharmonicities in the intermolecular potential.

Although they are not fully understood yet, the temporally two-dimensional Raman scattering results presented here provide valuable additional insight in liquid state dynamics that is not available in lower-order experiments. The analysis of the obtained signals gives clear indications for the directions of further improvement of our understanding of the liquid state.

ACKNOWLEDGMENTS

We would like to thank Professor G. R. Fleming, Professor Y. Tanimura, Dr. A. Tokmakoff, and Dr. K. Okumura for sending their preprints prior to publication, and are grateful to Dr. A. Tokmakoff and Dr. K. Tominaga for fruitful discussions. We acknowledge H. M. M. Hesp for his efforts to keep the copper-vapor laser operational. The investigations were supported by the Netherlands Foundations for Chemical Research (SON) and Physical Research (FOM) with financial aid from the Netherlands Organization for the Advancement of Science (NWO).

[1] W. J. Tomlinson, R. H. Stolen, and C. V. Shank, J. Opt. Soc. Am. B. **1**, 139 (1984).
[2] J. A. Valdmanis and R. L. Fork, IEEE J. Quantum Electron. **QE-22**, 112 (1986).
[3] F. Krausz, M. E. Fermann, T. Brabec, P. F. Curley, M. Hofer, M. H. Ober, C. Spielmann, E. Wintner, and A. J. Schmidt, IEEE J. Quantum Electron. **QE-28**, 2097 (1992).
[4] D. McMorrow, W. T. Lotshaw, and G. A. Kenney-Wallace, IEEE J. Quantum Electron. **QE-24**, 443 (1988).
[5] D. McMorrow and W. T. Lotshaw, J. Phys. Chem. **95**, 10 395 (1991).
[6] D. McMorrow, N. Thantu, J. S. Melinger, S. K. Kim, and W. T. Lotshaw, J. Phys. Chem. **100**, 10 389 (1996).
[7] S. Ruhman, L. R. Williams, A. G. Joly, and K. A. Nelson, J. Phys. Chem. **91**, 2237 (1987).
[8] A. Waldman, U. Banin, E. Rabani, and S. Ruhman, J. Phys. Chem. **96**, 10 842 (1992).
[9] R. F. Loring and S. Mukamel, J. Chem. Phys. **83**, 2116 (1985).
[10] B. J. Berne and R. Pecora, *Dynamic Light Scattering* (Wiley, New York, 1976).
[11] J. S. Friedman and C. Y. She, J. Chem. Phys. **99**, 4960 (1993).
[12] J. R. Klauder and P. W. Anderson, Phys. Rev. **125**, 912 (1962).
[13] R. Kubo, Advan. Chem. Phys. **15**, 101 (1969).
[14] P. C. Becker, H. L. Fragnito, J.-Y. Bigot, C. H. Brito-Cruz, R. L. Fork, and C. V. Shank, Phys. Rev. Lett. **63**, 505 (1989).
[15] E. T. J. Nibbering, D. A. Wiersma, and K. Duppen, Phys. Rev. Lett. **66**, 2464 (1991).
[16] D. Vanden Bout, L. J. Muller, and M. Berg, Phys. Rev. Lett. **43**, 3700 (1991).
[17] L. J. Muller, D. Vanden Bout, and M. Berg, J. Chem. Phys. **99**, 810 (1993).
[18] R. Inaba, K. Tominaga, M. Tasumi, K. A. Nelson, and K. Yoshihara, Chem. Phys. Lett. **211**, 183 (1993).
[19] D. P. Weitekamp, K. Duppen, and D. A. Wiersma, Chem. Phys. Lett. **102**, 139 (1983).
[20] K. Tominaga and K. Yoshihara, Phys. Rev. Lett. **76**, 987 (1996).
[21] M. Hoffmann and H. Graener, Chem. Phys. **206**, 129 (1996).
[22] Y. Tanimura and S. Mukamel, J. Chem. Phys. **99**, 9496 (1993).
[23] V. Khidekel and S. Mukamel, Chem. Phys. Lett. **240**, 304 (1995).
[24] T. Steffen, J. T. Fourkas, and K. Duppen, J. Chem. Phys. **105**, 7364 (1996).
[25] K. Tominaga and K. Yoshihara, Phys. Rev. Lett. **74**, 3061 (1995).
[26] K. Tominaga, G. P. Keogh, Y. Naitoh, and K. Yoshihara, J. Raman Spec. **26**, 495 (1995).
[27] K. Tominaga and K. Yoshihara, J. Chem. Phys. **104**, 1159 (1996).
[28] K. Tominaga and K. Yoshihara, J. Chem. Phys. **104**, 4419 (1996).
[29] T. Steffen and K. Duppen, in *Femtochemistry*, edited by M. Chergui (World Scientific, Singapore, 1996), p. 583.
[30] T. Steffen and K. Duppen, Phys. Rev. Lett. **76**, 1224 (1996).
[31] A. Tokmakoff and G. R. Fleming, J. Chem. Phys. (to be published).
[32] T. Steffen and K. Duppen (in preparation).
[33] E. T. J. Nibbering, K. Duppen, and D. A. Wiersma, J. Photochem. Photobio A Chem. **62**, 347 (1992).
[34] D. Frenkel and J. P. McTague, J. Chem. Phys. **72**, 2801 (1980).
[35] P. A. Madden and D. Kivelson, Adv. Chem. Phys. **87**, 191 (1987).
[36] L. C. Geiger and B. M. Ladanyi, J. Chem. Phys. **89**, 6588 (1988).
[37] S. Ruhman and K. Nelson, J. Chem. Phys. **94**, 859 (1991).
[38] D. McMorrow and W. T. Lotshaw, Chem. Phys. Lett. **201**, 369 (1993).
[39] J. Lukasik and J. Ducuing, Phys. Rev. Lett. **28**, 1155 (1972).
[40] R. K. Raj, Q. F. Gao, D. Bloch, and M. Ducloy, Opt. Commun. **51**, 117 (1984).
[41] J. E. Ivanecky and J. C. Wright, Chem. Phys. Lett. **206**, 437 (1993).
[42] The uncertainty in zero delay, associated with the replacement of the autocorrelation KDP crystal with the sample cuvet, is approximately 10–20 fs.
[43] N. E. Hill, Proc. Phys. Soc. (London) **82**, 723 (1963).
[44] R. M. Lynden-Bell and W. A. Steele, J. Chem. Phys. **94**, 859 (1991).
[45] A. Polimeno, G. J. Moro, and J. H. Freed, J. Chem. Phys. **102**, 8094 (1995).
[46] M. S. Pshenichnikov, K. Duppen, and D. A. Wiersma, Phys. Rev. Lett. **74**, 674 (1995).
[47] K. Okumura and Y. Tanimura, J. Chem. Phys. (submitted).